SDR-based Demonstration System and Applicability of SNR Aggregation for Multistage Distributed Cooperative Communication in MANETs

Mus'ab Yüksel
Hochschule Darmstadt
Darmstadt, Germany
musab.yueksel@h-da.de

Raphael T. L. Rolny
armasuisse Science and Technology
Thun, Switzerland
raphael.rolny@armasuisse.ch

Marc Kuhn
ZHAW
Winterthur, Switzerland
kumn@zhaw.ch

Michael Kuhn
Hochschule Darmstadt
Darmstadt, Germany
michael.kuhn@h-da.de

***Abstract*—Multistage or hierarchical distributed cooperative communication on the physical layer is a promising approach to overcome the scalability limitation of Mobile Ad-hoc Networks (MANETs). Standalone nodes that could successfully decode messages join transmission and support each other. They become a virtual transmit cluster and send simultaneously. While information theoretic research has demonstrated that an approximately linear scaling behaviour can be achieved, imperfections and constraints of practical systems have not been taken into account. Within this paper, we present a scalable and modular low-cost demonstration system based on software-defined radios (SDRs) to study distributed cooperative communication in practical MANETs. Furthermore, we apply SNR aggregation in combination with distributed cooperative transmission. To this end, we show a practical implementation approach and investigate the performance by measurements and simulations. Our results clearly highlight the advantages of combining distributed cooperative communication and SNR aggregation, e. g. to overcome larger distances in a distributed long haul multiple-input single-output (MISO) scenario or to enable a more efficient broadcast.**

***Index Terms*—MANET Scalability, Multistage Distributed Cooperative Broadcasting, Demonstration System, Software-Defined Radio (SDR), SNR Aggregation, Long Haul MISO**

I. Multistage Distributed Cooperative Communication in Mobile Ad-Hoc Networks

Mobile Ad-Hoc Networks (MANETs) are infrastructure-less and due to that commonly regarded as mission-critical and disaster-resistant. Thus, they can become particularly valuable for national authorities safety and security organizations in case of a blackout, e. g. after a natural catastrophe [1]. Besides, vehicular and flying MANETs (VANETs [2], FANETs [3]) gain a rising popularity nowadays. In ad-hoc networks often messages originated from one node have to be distributed in the entire network for network control and maintenance [4]. Moreover, safety critical messages have usually to be spread among all nodes. These kind of broadcasts build up a non-negligible amount of the overall network traffic and can cause performance bottlenecks [4]. Node movement and fast fading channels that particularly emerge for VANETs and FANETs cause frequent disconnections and rapid topology changes, which exacerbate the necessity for often broadcasts that common ad-hoc network routing protocols rely on [4]. Overall, it has to be stated, that MANETs currently suffer from a poor scalability [5].

Related information theoretic research has shown that *distributed cooperative communication* on the physical layer, where several standalone nodes send simultaneously, can enable an approximately linear scaling behaviour [5], [6], but did not consider impairments and constraints of practical systems. In fact, ideal cooperation is presumed, where each sending node's contribution can be perfectly considered. However, real-world systems suffer from imperfections due to hardware limitations. Besides, specific impairments arise due to aggregating several standalone nodes to a virtual transmit cluster, such as multiple carrier frequency and timing offsets [7], [8].

Transmit diversity schemes, e. g. Space-Time Block-Codes (STBCs), allow for a comparably low-complexity implementation of cooperative communication [1]. Collisions, provoked by the simultaneously sending active nodes are not harmful, but purposely exploited [1]. Nonetheless, adaptations are necessary to utilize them for distributed setups [1]. Recently, a single-carrier (time-domain equalization) [7] and multi-carrier (OFDM) [8] communication system for distributed cooperative communication have been proposed that are tailored to the needs of practical systems and the associated impairments. Both systems utilize STBCs, in particular Linear-Scalable Dispersion Codes (LSDCs) [9], which allow to profit from both, distributed transmit diversity and SNR gain. The transmit diversity encoding ensures that the superposition is always constructive, i. e. catastrophic destructive interference is avoided, at the cost of suppressing coherent interference as well [1], [10].

We utilize this approach to enhance the performance of broadcasting in practical MANETs. In a *multistage (or hierarchical) distributed cooperative broadcast* [5], [6] scenario one node starts to send. Surrounding nodes, that were able to successfully decode, join transmission and participate in distributing the message. Decoding success can be assumed e. g. if the cyclic redundancy check (CRC) of a forward error correcting (FEC) scheme is fulfilled or if the signal-to-noise ratio (SNR) is above a certain threshold. Nodes, that were able to decode

This is the author's accepted manuscript version of a paper published by IEEE. The Version of Record is available at IEEE *Xplore*: https://doi.org/10.1109/VTC2023-Spring57618.2023.10199930

retain active, i. e. send repeatedly, until the complete network is covered, wherefore the number of transmitting nodes is gradually increased for each broadcast stage. The growing number of TX typically enables to cover larger distances, which can be valuable in a *distributed long haul multiple-input single-output (MISO)* scenario, where several nearby nodes, i. e. a virtual TX cluster, try or, respectively tries to reach a distant receiver [5].

SNR aggregation, also referred to as *accumulative broadcast*, is a further low-complexity strategy to improve the performance, especially in the portrayed distributed multistage broadcast and long haul MISO scenario [6], [10]. Nodes, that cannot decode the message at the early stages can store these observations instead of discarding the packets. Accordingly, continuously aggregating all arriving packets facilitates to increase the reliability of decoding which in turn can allow to reduce the communication delay.

Contributions

The scalability of MANETs is one major concern for a widespread implementation. Theoretic concepts introduced multistage (hierarchical) distributed cooperative communication as an approach that can overcome this limitation [5], [6], [10]. However, imperfections of practical systems due to hardware constraints and due to the aggregation of several nodes to a virtual MISO system are not considered therein. In our previous research, we introduced communication systems that particularly concentrate on these [7], [8]. Within this paper, we present a scalable and modular low-cost demonstration system based on software-defined radios (SDRs) that enables to investigate distributed multistage cooperative communication (broadcasting) in practical MANETs. To the best of our knowledge, it is the first of its kind. To enhance the performance of the systems presented in [7], [8], we investigate the applicability of SNR aggregation and propose an implementation approach. We investigate the benefits of combining SNR aggregation with distributed cooperative transmission by means of measurements and simulations. Our evaluations clearly indicate, that the proposed combination is conspicuously advantageous to overcome larger distances and isolation in a distributed long haul MISO scenario.

For the remainder, x denotes a scalar, $\mathbf{x}$ a vector, $\mathbf{X}$ a matrix and $\ddot{\mathbf{X}}$ a diagonal matrix where $\mathbf{X}(i,j) = 0$ for $i \neq j$. Additionally, $(\cdot)^H$ refers to the adjoint (complex transpose).

II. System Model

This paper is grounded on the recently proposed single-carrier (time-domain equalization) communication system for distributed cooperative transmission as described in [7]. The input symbol vector $\boldsymbol{\alpha} \in \mathbb{C}^{N_\mathrm{I},1}$ contains N_I 4-QAM symbols and is first encoded with a numerically optimized outer code matrix $\mathbf{R} \in \mathbb{C}^{N_\mathrm{C},N_\mathrm{C}}$, where N_C refers to the encoded block length. Thereby, a higher modulation order can be selected at any time. To obtain the specific transmit signals, each node performs a multiplication with a random phase inner code $\ddot{\mathbf{C}}_{\mathrm{TX,i}}$. Hence, the transmit signal for the i-th node can be expressed by $\mathbf{u}_{\mathrm{TX,i}} = \ddot{\mathbf{C}}_{\mathrm{TX,i}} \cdot \mathbf{R} \cdot \boldsymbol{\alpha}$. On that account, each node sends the same information but a different signal, whereas destructive interference is avoided due to the transmit diversity encoding.

For each link, the transmission considering the channel state and carrier frequency offset (CFO) can be summarized by a transmit property matrix

$$\mathbf{Q}_{\mathrm{TX,i}} = \ddot{\mathbf{C}}_{\mathrm{TX,i}} \cdot \mathbf{H}^{\Theta}_{\mathrm{TX,i}} \cdot \ddot{\boldsymbol{\Phi}}_{\mathrm{TX,i}},\ \mathbf{Q}_{\mathrm{TX,i}} \in \mathbb{C}^{N_\mathrm{C},N_\mathrm{C}}, \tag{1}$$

where $\mathbf{H}^{\Theta}_{\mathrm{TX,i}} \in \mathbb{C}^{N_\mathrm{C},N_\mathrm{C}}$ is a channel state convolution matrix and $\ddot{\boldsymbol{\Phi}}_{\mathrm{TX,i}} \in \mathbb{C}^{N_\mathrm{C},N_\mathrm{C}}$ is a diagonal matrix related to the node's CFO. The overall transmission property matrix can be expressed by $\mathbf{Q} = \sum_{i=1}^{N_\mathrm{TX}} \mathbf{Q}_{\mathrm{TX,i}}, \mathbf{Q} \in \mathbb{C}^{N_\mathrm{C},N_\mathrm{C}}$.

At the RX, a matched multiplication is performed, so that the matched received symbol vector is obtained by

$$\mathbf{y}_\mathrm{m} = \mathbf{R}^H \cdot \mathbf{Q}^H \cdot \mathbf{y},\ \mathbf{y}_\mathrm{m} \in \mathbb{C}^{N_\mathrm{C},1}, \tag{2}$$

where $\mathbf{y} \in \mathbb{C}^{N_\mathrm{C},1}$ refers to the received symbol vector. Correspondingly, the summarizing correlation matrix immediately follows as

$$\boldsymbol{\Lambda} = \mathbf{R}^H \cdot \mathbf{Q}^H \cdot \mathbf{Q} \cdot \mathbf{R},\ \boldsymbol{\Lambda} \in \mathbb{C}^{N_\mathrm{C},N_\mathrm{C}}, \tag{3}$$

$$\text{so that } \mathbf{y}_\mathrm{m} = \boldsymbol{\Lambda} \cdot \boldsymbol{\alpha}. \tag{4}$$

III. Demonstration System Architecture

Our main objective is to design a scalable and modular architecture that on the one hand allows to arbitrarily add nodes and that on the other hand retains the computational effort at the controlling PCs manageable. To this end, we decide for a network based solution which allows to shift the computational complexity to the edge. For our concrete setup, we employ Raspberry Pi 4 (RasPi) computers as edge computing devices to control all SDRs dedicated for transmission. Besides, we rely on Windows computers to operate SDRs that receive packets. The employed Ettus Research B210 SDRs possess two decoupled RF chains. We make use of this property to

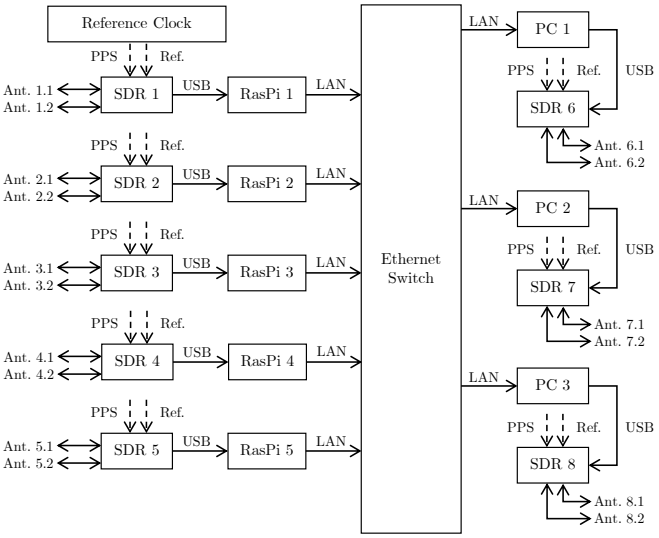

Fig. 1: Presented demo system architecture

ease the system setup and to minimize the necessary amount of devices in order to keep the complexity and costs as low as possible. Since we however do not want to investigate the behaviour for co-located, but for distributed nodes, we connect each SDR output via cables to appropriate antennas with stands. These are mounted on magnetic platelets, which allows us to flexibly modify the exact position and by that the topology of the emulated MANET. Extending the system to utilize receive diversity by employing two antennas is straightforward. To minimize the impact of unwanted deviations and impairments, we additionally employ an Ettus Research Octoclock that provides a pulse-per-second (PPS) and 10 MHz reference clock. All SDRs are connected via USB to either a RasPi or a Windows PC, whereas all RasPis and PCs are member of a private IP network.

Fig. 1 illustrates the described architecture. Supplementary, Fig. 2 provides an impression of the concrete setup of the reference clock, network switch, SDRs and RasPis.

Fig. 2: Reference clock, network switch, TX SDRs and RasPis

A. Programming Interfaces

The user, i. e. the operator of the demo system is able to start, monitor and evaluate the measurements from a single PC (operator PC). All remaining devices can be configured remotely by the latter. For the RX SDRs, the C/C++ interface is utilized, whereas the API is embedded into Matlab via mex files. In contrast, each RasPi accesses the TX SDRs via the Python API. This inter-dependency is visualized in Fig. 3.

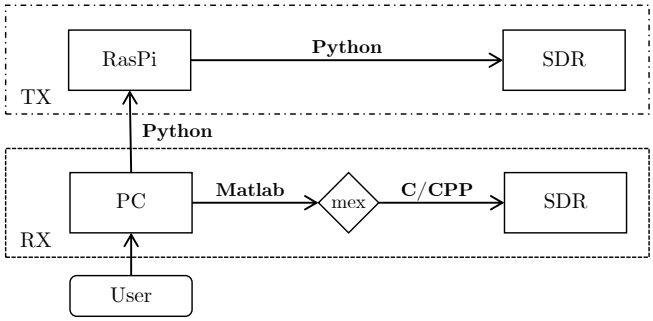

Fig. 3: Inter-dependency of programming interfaces (APIs)

B. Modularity

Right from the beginning, we focused on a strict modularity. Consistently, several *modules* can be identified in our system ('Time Synchronization', 'Parameter Estimation', 'Channel Model', 'Interference Decoder', 'Antenna Placement / Network Topology', 'Number of Transmitting Nodes N_{TX}', 'Number of Receiving Nodes N_{RX}'), where each component of our demo system is easily interchangeable or, respectively, expandable. Thus, our system is also a perfect testbed to study the performance of various approaches that fulfil the same task, e. g. channel state estimation (see Section III-C).

C. Channel State Estimation

We primarily concentrate on the behaviour of cooperative transmission and SNR aggregation. Hence, the channel estimation is of minor importance with its main purpose being to ensure that the channel state is determined as accurate as possible. Ideally, the quality of estimation should be the same for each link. Therefore, it appears reasonable to use sequential training for our setup. Thus, the training sequences for each link are transmitted one after the other, while all nodes send the payload data simultaneously. This burst structure is depicted in Fig. 4. Thereby, we use a Zadoff-Chu sequence of length $L_{\mathrm{ZC}} = 61$ and root $R_{\mathrm{ZC}} = 12$ for time synchronization and a maximum-length sequence (m-sequence) of length $L_{\mathrm{mSeq}} = 31$ for the channel state estimation of each link.

Although sequential training is not very efficient, we stick

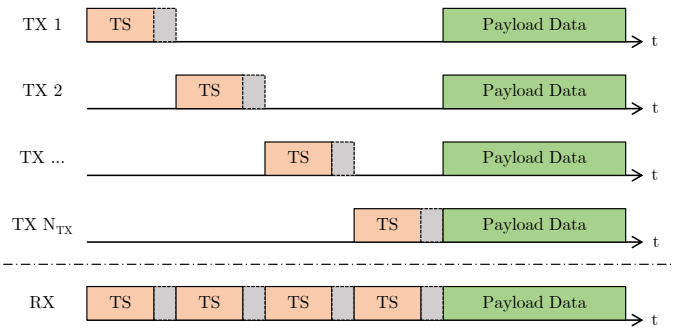

Fig. 4: Implemented burst structure for sequential training

with this approach to verify the concept of our demo system

and SNR aggregation. The demo system's modularity can be utilized to interchange the sequential implementation with concurrent estimation techniques, whose feasibility has been demonstrated in related research, e. g. in [11], at any time. Accordingly, constraints to the scalability because of the parameter estimation can be avoided.

D. Measurement Protocol

As soon as the RX nodes begin receiving, we consider a measurement to have started. For each measurement iteration (packet reception), first a previously specified number of samples is received, i. e. the RX buffer is filled. Thereafter, a time synchronization is performed. After detecting the start of the frame (SOF), the training sequences are extracted in order to perform a channel estimation for each link. Next, the payload data is decoded using the obtained channel state information.

E. Antenna Placement

In a real-world system, the distances between the communicating nodes are typically comparably large with respect to the carrier wavelength λ_c. However, the situation differs for our demo system, where we deploy an indoor setup with comparably small distances. Hence, the nodes have to be placed with some care to avoid any nearfield and antenna coupling effects. For electrically small antennas, the distances between the nodes should be much larger than λ_c. Accordingly, we select a carrier frequency of $f_\mathrm{c} = 2.8$ GHz, so that $\lambda_\mathrm{c} \approx 10.71$ cm. Based on this choice, we place all nodes such that the minimum distance between them is typically larger than 80 cm $\approx 8 \cdot \lambda_\mathrm{c}$.

F. Channel Model

In our indoor lab environment, the channels between the transmitting and receiving nodes are dominated by a strong line-of-sight (LOS) component. The delay spread is comparably small with respect to the symbol duration. The attenuation is majorly determined by the node placement and thus the path-loss for that particular link, wherefore it is relatively static. In order to perform measurements in a more dynamic environment, we artificially introduce Rayleigh fading for selected measurements by manipulating the transmit signals accordingly in advance. This approach has the side effect that we can use the same fading characteristics repeatedly. In total, we can perform measurements in both, a static strongly LOS-dominated as well as a more dynamic Rayleigh fading environment, whereas the distance-dependent path-loss likewise affects both.

G. SNR Regime

We vary the SNR at the RX and perform measurements in a rather 'low' SNR regime (range approximately -5 to +5 dB) which allows us to detect an expressive BER level for a reasonable number of transmissions. The SNR is set by appropriately scaling the transmit power for the payload data. Conversely, the transmit power for the sequential training sequences is not reduced at any time to ensure the same quality of channel estimation and synchronization for all measurements.

IV. SNR Aggregation

During a typical broadcast scenario, the same message is transmitted repeatedly by many different nodes. Accordingly, receiving nodes are able to observe multiple copies. These observations can be aggregated to increase the reliability of decoding (*SNR aggregation*). In a distributed cooperative transmission setup, several nodes send simultaneously. Because of that, receiving nodes can aggregate packets which already constitute a superposition of all the active nodes' transmit signals. Therefore, the combination of distributed cooperative transmission and SNR aggregation during a multistage cooperative broadcast is particularly advantageous.
For our particular system, the equivalent model for the aggregated packets can be expressed by $\mathbf{y}_\mathrm{agr} = \mathbf{\Lambda}_\mathrm{agr} \cdot \boldsymbol{\alpha}$.
$\mathbf{\Lambda}_\mathrm{agr}$ and $\mathbf{y}_\mathrm{agr}$ are representing the superposition of several observations N_agr. So,

$$\mathbf{\Lambda}_\mathrm{agr} = \sum_{i=1}^{N_\mathrm{agr}} \mathbf{\Lambda}_\mathrm{i} = \sum_{i=1}^{N_\mathrm{agr}} \mathbf{R}^H \cdot \left[\sum_{i=1}^{N_\mathrm{TX}} \mathbf{Q}_\mathrm{TX,i}\right]^H \cdot \left[\sum_{i=1}^{N_\mathrm{TX}} \mathbf{Q}_\mathrm{TX,i}\right] \cdot \mathbf{R} \tag{5}$$

and

$$\mathbf{y}_\mathrm{agr} = \sum_{i=1}^{N_\mathrm{agr}} \mathbf{y}_\mathrm{m,i} = \sum_{i=1}^{N_\mathrm{agr}} \mathbf{R}^H \cdot \left[\sum_{i=1}^{N_\mathrm{TX}} \mathbf{Q}_\mathrm{TX,i}\right]^H \cdot \mathbf{y}, \tag{6}$$

where $\mathbf{\Lambda}_\mathrm{i}$ and $\mathbf{y}_\mathrm{m,i}$ refer to the correlation matrix $\mathbf{\Lambda}$ and matched received symbol vector $\mathbf{y}_\mathrm{m}$ of the i-th observation. N_agr denotes the aggregation group size.

The herein presented approach constitutes a temporal

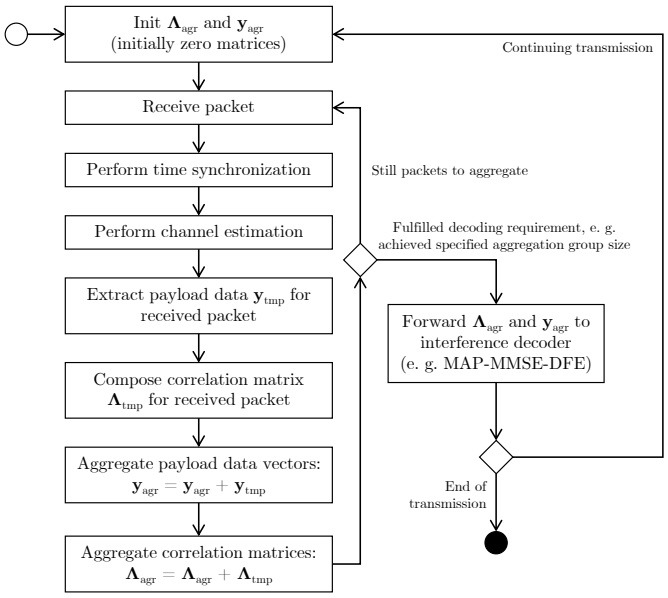

Fig. 5: SNR aggregation: Implementation

maximum-ratio combining (T-MRC), whose implementation

is shown in Fig. 5. Considering our demo system, SNR aggregation is not performed in real time during a measurement but afterwards to enable various and more flexible evaluations with the exact same packets. In a practical system, SNR aggregation can be performed for an a-priori defined fixed number of observations, as long as the SNR of the aggregated packet is below a predefined SNR threshold or as long as the CRC of a FEC scheme fails. For our studies, we rely on an iterative MAP-MMSE-DFE decoder [12].

Scenarios

Basically, we investigate SNR aggregation in two different scenarios which vary in their node distribution.
First, we arbitrarily place transmitting nodes rather dense around receiving nodes, while the link quality changes according to previously defined Rayleigh fading coefficients for each packet. An exemplary setup is shown in Fig. 6, whereas the depicted fading characteristics denote a snapshot in time. We vary the number of active nodes N_{TX} and investigate the decoding performance for varying N_{aggr}. It is important to recall that N_{TX} is constant throughout the aggregation process. Although this scenario does not immediately correspond to the propagation of a message (it can be rather regarded as an intermediate snapshot during a broadcast), it is particularly suited to highlight the impact of N_{TX} and N_{aggr}.

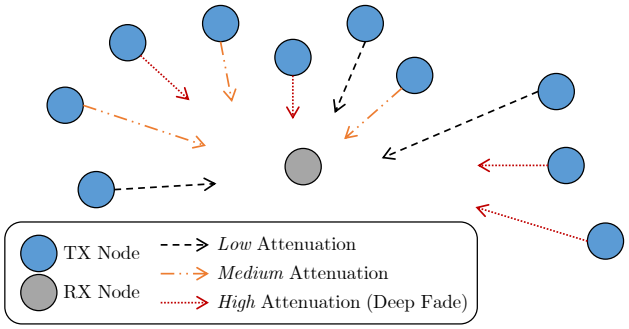

Fig. 6: *Dense network* scenario, constant N_{TX} throughout aggregation

Next, we pay attention to the distributed long haul MISO scenario. One node starts to send, whereas the isolated node receives a highly attenuated packet that it would normally discard in a non-aggregation scenario. Adjacent nodes, i. e. nodes located nearby to the initially sending node receive messages, too, of which some will be able to successfully decode. Those join the transmission, so that in the next time slot or broadcast stage the isolated node receives the superimposed packet of all active nodes, which probably is still highly attenuated. Again, some nearby nodes will be able to successfully decode. The latter build a virtual transmit cluster, while the isolated node continuously aggregates all packets, that it receives. In contrast to aforementioned scenario, the number of transmitting nodes is steadily rising during aggregation, which directly corresponds to the typical propagation of a message within a MANET (multistage distributed cooperative broadcasting) [1], [7], [8]. Fig. 7 shows a typical configuration. For our measurements or evaluations in the first broadcast stage 1 TX, in the second stage 2 TX, in the third stage 4 TX, in the fourth stage 6 TX, in the fifth stage 8 TX and lastly in the sixth stage 10 TX are active, just as depicted in the figure. We investigate the behaviour after each stage for varying N_{aggr} where the latter indicates the number of observations per stage in this context. E. g. $N_{\text{aggr}} = 2$ means, that 2 packets are always aggregated when 1 TX, 2 TX, 4 TX, 6 TX, 8 TX and 10 TX are active, so that for this specific example in total 12 packets are utilized.

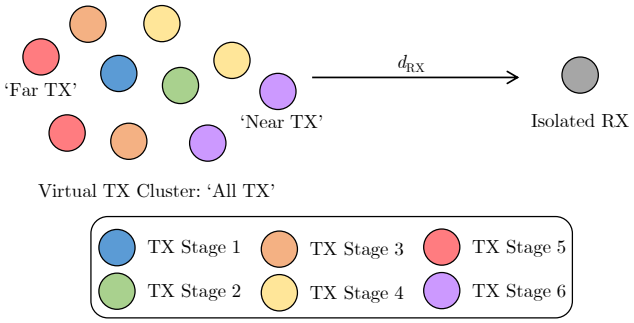

Fig. 7: *Long haul MISO* scenario, gradually increasing N_{TX} during aggregation

V. Measurement Results

Prior to discussing the results obtained in presence of artificial Rayleigh fading, we want to express the benefits of cooperative transmission and SNR aggregation first in a *static* LOS-dominated environment. For that, we consider the MANET topology depicted in Fig. 7. In a classical non-cooperative multihop scenario, a *far* away node could start transmission aiming to reach the isolated node. To this end, the message will be forwarded within the cluster until the *nearest* or *best positioned* node is reached that finally tries to reach the isolated RX. Contrary, in a classical cooperative approach, all TX of the cluster simultaneously send and support each other. We study the necessary number of aggregated packets to achieve certain BER levels (see Fig. 8). It is on hand, that a tremendously high N_{aggr} is required if solely the far node is active ($N_{\text{aggr}} = 766$). That being the case, only the first BER margin of 10^{-1} can be reached with the recorded amount of packets, wherefore the diagram correspondingly only depicts a single bar. The performance gets significantly better, once the near node is sending, which denotes the gain of multihop communication. Comparing the necessary number of arriving packets to achieve the first margin of interest which is 10^{-1}, N_{aggr} can be lowered to 7. To accomplish lower BER levels, N_{aggr} is accordingly higher. A major performance boost is further possible with cooperative transmission. Distinctly less packets have to be aggregated to achieve the same margins. N_{aggr} can be lowered approximately to $1/3$ for $\mu_{\text{BER}} = 10^{-1} \ldots 10^{-3}$ and to $1/2$ for $\mu_{\text{BER}} = 10^{-5} \ldots 10^{-6}$.

We want to explicitly state that we do not concentrate on the propagation of a message *within* the cluster and focus on the mentioned edge cases to point out the behavioural differences.

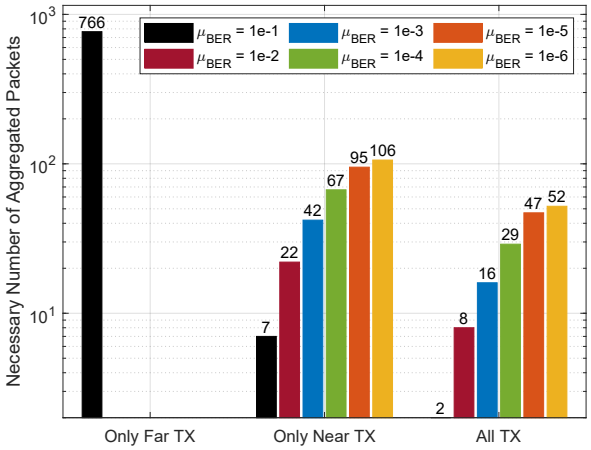

Fig. 8: Necessary number of aggregated packets to achieve certain BER levels if only the far, near (best positioned) or all TX are active; static setup with LOS paths

Next, we regard the first scenario with artificial Rayleigh fading where N_{TX} retains constant throughout the aggregation process. It becomes obvious that μ_{BER} gets the lower, the higher N_{agr} and the higher N_{TX} get (see Fig. 9). Starting from a relatively high BER level (approximately $2...5 \cdot 10^{-1}$), it attracts attention that a relatively small N_{agr} is sufficient to undershoot levels of 10^{-2} or 10^{-3} if N_{TX} is enlarged, e. g. $N_{\text{aggr}} = 5$ if $N_{\text{TX}} = 8$ for $\mu_{\text{BER}} = 10^{-2}$. The communication delay, i. e. the time until all nodes dedicated for transmission send their corresponding message, is below that of classical non-cooperative multi-hop communication as long as $N_{\text{agr}} \leq N_{\text{TX}} - 1$. Accordingly, combining SNR aggregation and distributed cooperative transmission typically does not require more channel uses than non-cooperative multi-hop communication, while significantly lower BER levels can be achieved. Therefore, it is a low-complexity approach to distinctly increase the performance, which still allows to reduce the communication delay for an appropriate protocol. E. g. considering a transmission case with $N_{\text{TX}} = 8$, 8 time-slots or, respectively, channel uses would be necessary in a classical non-cooperative multi-hop communication to allow each node to send once. Thereby, the BER is probably still very high (see results for $N_{\text{TX}} = 1$). In contrast, $N_{\text{agr}} = 5$ is sufficient to reduce the mean BER from 0.177 to approximately $10^{-2} = 0.01$. This ratio between N_{agr} and the communication delay gets the better, the higher N_{TX} is.

Succeeding, we focus on the *'long haul MISO'* scenario in a Rayleigh fading environment (see Fig. 10). It becomes immediately clear, that SNR aggregation allows to reduce the BER drastically, especially for a slightly increased N_{aggr}. Considering a specific BER threshold to detect decoding success, the broadcast can be regarded to succeed conspicuously

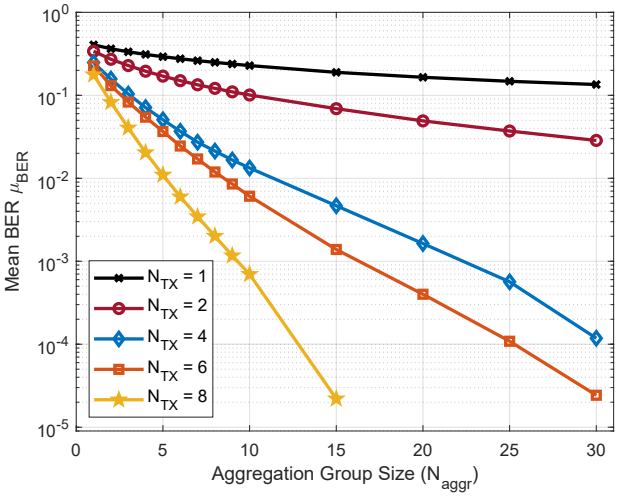

Fig. 9: μ_{BER} for varying N_{TX} and N_{agr}, constant N_{TX} throughout aggregation, Rayleigh fading environment

earlier. E. g. arbitrarily presuming $\mu_{\text{BER}} = 10^{-1}$ as decoding boundary, the network is covered after the third stage if $N_{\text{aggr}} = 16$, the fourth stage if $N_{\text{aggr}} = 8$, the fifth stage if $N_{\text{aggr}} = 4$ and finally the sixth stage if $N_{\text{aggr}} = 2$. From a different perspective, a tradeoff is possible between the involved number of TX which increases with each broadcast stage and the number of transmissions with a limited number of TX (enhanced N_{aggr}).

Lastly, we compare the results obtained by measurements to those achievable with simulations to check the performance of our demo system. Fig. 10 immediately reveals, that the simulation results highly correspond to the measurement results. Of course, there are some small differences in the specific values reasoned in deviating transmit power levels and varying distances between the TX and RX.

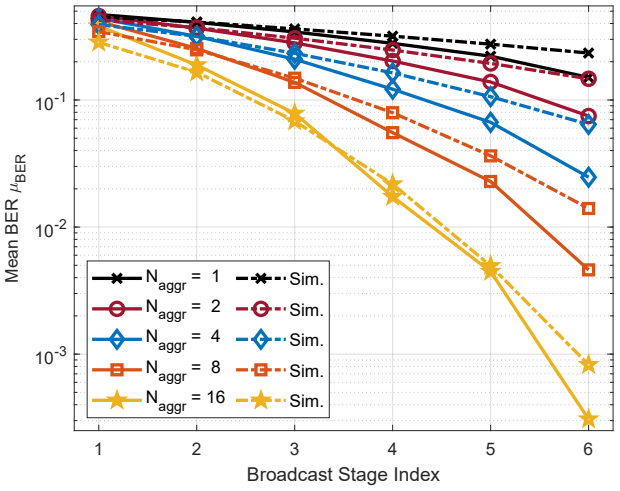

Fig. 10: μ_{BER} after each broadcast stage for varying N_{aggr}, gradually increased N_{TX} for each stage, Rayleigh-fading environment, comparison of measurement and simulation results

Based on all these observations, it can be concluded that while SNR aggregation and distributed cooperative communication by itself allow to increase the transmission robustness, the combination of both is particularly beneficial in a multi-stage distributed broadcast scenario.

Especially worth mentioning are the benefits in a *'long haul MISO'* situation. Instead of requiring retransmissions as packets with low SNR and high BER are typically discarded without aggregation, the necessity of retransmissions is reduced, as in this case *early* arriving packets are utilized for aggregation. From a different perspective, often isolated or far away nodes are not expected to decode the message in the first broadcast stages. However, SNR aggregation can enable exactly this which can empower an even lower communication delay as it is already the case when employing cooperative transmission. Therefore, the herein presented combination of cooperative transmission and SNR aggregation constitutes a low-complexity option for long-distance communication compared to coherent distributed transmission schemes that are of higher complexity and most probably not as robust as the presented approach.

It is noteworthy that comparably low N_{aggr} must not necessarily be related to incoming packets in consecutive time slots. In fact, it is conceivable, that some observations are recorded simultaneously with multiple antennas at one node (receive diversity), which would lead to a distinct performance advantage while retaining the communication delay low.

However, it should be emphasized that we presuppose perfect (for our simulations) or at least a very exact knowledge (for our measurements) about the channel state. While aggregation is especially useful if the SNR at the RX is comparably low, further considerations about the parameter estimation are required in this SNR regime, wherefore the quality of estimation can become the limiting factor. We suggest to systematically investigate the impact of imperfect channel estimation on the performance in future research.

VI. Conclusion

We presented a scalable and modular low-cost SDR-based demonstration system to study distributed multistage cooperative communication in practical MANETs. Due to its architecture and design our demo system is a fruitful, easily expandable and flexibly adaptable tool.

Furthermore, we enhanced the performance of previously introduced cooperative communication systems by exploiting SNR aggregation, for which we introduce a practical implementation approach.

Our measurements clearly showed the benefits of combining SNR aggregation and distributed cooperative communication. Aiming to deploy cooperative communication in MANETs, this is beneficial for a physical layer communication protocol, specifically for mission-critical networks that have to be particularly robust.

Acknowledgment

This research work has been funded by *armasuisse Science and Technology*.

References

[1] M. Yüksel, R. Rolny, M. Kuhn, and M. Kuhn, "Applicability of space-time block codes for distributed cooperative broadcasting in manets with high node mobility," *IEEE 95th Vehicular Tech. Conf. VTC Spring*, 2022.

[2] T. K. Bhatia, R. K. Ramachandran, R. Doss, and L. Pan, "A comprehensive review on the vehicular ad-hoc networks," *IEEE 8th Int. Conf. on Reliability, Infocom Technologies and Optimization (ICRITO)*, 2020.

[3] J. Lin, W. Cai, S. Zhang, X. Fan, S. Guo, and J. Dai, "A survey of flying ad-hoc networks: Characteristics and challenges," *IEEE 8th Int. Conf. on Instr. Meas., Computer, Comm. and Control (IMCCC)*, 2018.

[4] G. Kaur and P. Thakur, "Routing protocols in manet: An overview," *IEEE 2nd Int. Conf. on Intelligent Computing, Instr. and Control Technologies (ICICICT)*, 2019.

[5] A. Özgür, O. Lévêque, and D. Tse, "Beyond multi-hop: Optimal cooperation in large wireless networks," in *2010 Proceedings of 19th Int. Conf. on Computer Comm. and Networks*, pp. 1–6, 2010.

[6] B. Sirkeci-Mergen, A. Scaglione, and G. Mergen, "Asymptotic analysis of multistage cooperative broadcast in wireless networks," *IEEE Transactions on Information Theory*, vol. 52, no. 6, pp. 2531–2550, 2006.

[7] M. Yüksel, R. Rolny, M. Kuhn, and M. Kuhn, "Distributed cooperative transmission in manets with multiple timing and carrier frequency offsets," *IEEE 33rd Annual Int. Symposium on Personal, Indoor and Mobile Radio Comm. (PIMRC)*, 2022.

[8] M. Yüksel, R. Rolny, M. Kuhn, and M. Kuhn, "Multi-carrier (ofdm) cooperative transmission in manets with multiple carrier frequency offsets," *IEEE 18th Int. Conf. on Wireless and Mobile Computing, Networking and Comm.*, 2022.

[9] A. Wittneben and M. Kuhn, "A new concatenated linear high rate space-time block code," *IEEE 55th Vehicular Tech. Conf. VTC Spring*, 2002.

[10] K. Vardhe and D. Reynolds, "The performance of multistage cooperation in relay networks," *Journal of Communications and Networks*, vol. 17, no. 5, pp. 499–505, 2015.

[11] E. Keramat, N. Kauffroath, K. Karbasi, H. Zhao, B. Daneshrad, and G. Pottie, "Experimental results for low overhead frequency offset estimation in manets with concurrent transmission," *IEEE MILCOM*, 2017.

[12] M. Kuhn and A. Wittneben, "A new scalable decoder for linear space-time block codes with intersymbol interference," *IEEE 55th Vehicular Tech. Conf. VTC Spring*, 2002.